AMERICAN SOCIETY FOR MICROBIOLOGY | Journal of Virology®

VACCINES AND ANTIVIRAL AGENTS

Enhancement of HIV-1 Env-Specific CD8 T Cell Responses Using Interferon-Stimulated Gene 15 as an Immune Adjuvant

Carmen Elena Gómez,[a] Beatriz Perdiguero,[a,b] Michela Falqui,[b] María Q. Marín,[a] Martina Bécares,[b] Carlos Óscar S. Sorzano,[c] Juan García-Arriaza,[a] Mariano Esteban,[a] Susana Guerra[b]

[a]Department of Molecular and Cellular Biology, Centro Nacional de Biotecnología, CSIC, Madrid, Spain
[b]Department of Preventive Medicine and Public Health and Microbiology, Universidad Autónoma de Madrid, Madrid, Spain
[c]Biocomputing Unit and Computational Genomics, Centro Nacional de Biotecnología, CSIC, Madrid, Spain

ABSTRACT Induction of the endogenous innate immune system by interferon (IFN) triggers the expression of many proteins that serve like alarm bells in the body, activating an immune response. After a viral infection, one of the genes activated by IFN induction is the IFN-stimulated gene 15 (*ISG15*), which encodes a ubiquitin-like protein that undergoes a reversible posttranslational modification (ISGylation). ISG15 protein can also act unconjugated, intracellularly and secreted, acting as a cytokine. Although ISG15 has an essential role in host defense responses to microbial infection, its role as an immunomodulator in the vaccine field remains to be defined. In this investigation, we showed that ISG15 exerts an immunomodulatory role in human immunodeficiency virus (HIV) vaccines. In mice, after priming with a DNA-ISG15 vector mixed with a DNA expressing HIV-1 gp120 (DNA-gp120), followed by a booster with a modified vaccinia virus Ankara (MVA) vector expressing HIV-1 antigens, both wild-type ISG15-conjugated (ISG15-wt) and mutant unconjugated (ISG15-mut) proteins act as immune adjuvants by increasing the magnitude and quality of HIV-1-specific CD8 T cells, with ISG15-wt providing better immunostimulatory activity than ISG15-mut. The HIV-1 Env-specific CD8 T cell responses showed a predominant T effector memory (TEM) phenotype in all groups. Moreover, the amount of DNA-gp120 used to immunize mice could be reduced 5-fold after mixing with DNA-ISG15 without affecting the potency and the quality of the HIV-1 Env-specific immune responses. Our study clearly highlights the potential use of the IFN-induced ISG15 protein as immune adjuvant to enhance immune responses to HIV antigens, suggesting that this molecule might be exploitable for prophylactic and therapeutic vaccine approaches against pathogens.

IMPORTANCE Our study described the potential role of ISG15 as an immunomodulatory molecule in the optimization of HIV/AIDS vaccine candidates. Using a DNA prime–MVA boost immunization protocol, our results indicated an increase in the potency and the quality of the HIV-1 Env-specific CD8 T cell response. These results highlight the adjuvant potency of ISG15 to elicit improved viral antigen presentation to the immune system, resulting in an enhanced HIV-1 vaccine immune response. The DNA-ISG15 vector could find applicability in the vaccine field in combination with other nucleic acid-based vector vaccines.

KEYWORDS ISG15 adjuvant, alarmin, DNA vectors, MVA-B, HIV vaccine, immune responses, ISG15, vaccines

The recent coronavirus pandemic highlights how important for humanity is the development of effective vaccines that protect us from emerging virus infection outbreaks, which can cause the deaths of hundreds of thousands of people and have a high impact on the global economy. Before the introduction of vaccines in public

Citation Gómez CE, Perdiguero B, Falqui M, Marín MQ, Bécares M, Sorzano CÓS, García-Arriaza J, Esteban M, Guerra S. 2021. Enhancement of HIV-1 Env-specific CD8 T cell responses using interferon-stimulated gene 15 as an immune adjuvant. J Virol 95:e01155-20. https://doi.org/10.1128/JVI.01155-20.

Editor Viviana Simon, Icahn School of Medicine at Mount Sinai

Address correspondence to Carmen Elena Gómez, cegomez@cnb.csic.es, or Susana Guerra, susana.guerra@uam.es.

Received 8 June 2020
Accepted 21 October 2020
Accepted manuscript posted online 28 October 2020
Published 22 December 2020

health, natural immunity was the only mechanism that protected people from viral infections, and hence, understanding the immune responses and signaling pathways involved in this mechanism is fundamental for the development of effective vaccines. Over the past few years, our knowledge about the processes that regulate protective immunity has rapidly expanded, while there are still many unidentified molecular aspects, which are essential to further improve current vaccination strategies. For this reason, future studies covering the remaining gaps in these signaling pathways will be crucial in the biomedical field.

After a viral infection, the host's innate immune system and interferon (IFN) induction are an essential first-line defense to prevent viral replication before a more specific protection induced by the adaptive immune system is elicited. Host pattern recognition receptors (PRRs) recognize viral components triggering several signaling pathways that ultimately lead to the production of type I IFN, responsible for the transcriptional induction of a large group of genes called interferon-stimulated genes (ISGs), which are indispensable elements for host resistance to viral infections and for generation of the antiviral state. One of the most highly induced genes in the type I IFN signaling pathway is *ISG15*, which encodes a small ubiquitin-like (Ubl) protein involved in a posttranslational modification process known as ISGylation. ISGylation is a reversible protein modification that involves a cascade of enzymatic reactions that finally bind ISG15 to a lysine residue of *de novo*-synthesized target proteins (1–4). The isopeptidase ubiquitin-specific protease 18 (USP18) is the specific enzyme involved in the release of ISG15 from the ISGylated protein. In mice, a mutation of the USP18 protein (USP18-C61A) completely abolishes the isopeptidase activity, producing excessive ISGylation, which blocks viral infection (5).

The role of ISGylation is not exclusive to viral or bacterial infections, but the implication of ISGylation in processes such as cancer progression (6), metabolism control after infection (7–9), hypoxia response (10), or exosome secretion (3), among many others, has recently been elucidated. In addition to the presence of conjugated ISG15, ISG15 protein can be found as a free molecule in two different states: intracellular and extracellular, acting as a cytokine. Although our knowledge of ISGylation has increased greatly in the last years, the role of free ISG15 as an extracellular cytokine is less known. Lymphocyte function-associated antigen 1 receptor (LFA1), the classical receptor for intercellular adhesion molecule 1 (ICAM-1), has been identified as the cellular receptor for ISG15, promoting IFN-γ and interleukin-10 (IL-10) secretion in natural killer (NK) cells (11). In humans, intracellular ISG15 is essential to prevent IFN-α/β overamplification (12). The role of ISG15 as an inductor of IFN-γ secretion seems to be the basis for the increased susceptibility to mycobacterial diseases in human patients lacking a functional form of ISG15 (13). Secreted ISG15 has also been described to promote NK cell (14) and dendritic cell (DC) (15) maturation and to act as a chemotactic factor for neutrophils (16). During parasite infection, the presence of dimeric and multimeric forms of extracellular ISG15 is important for its cytokine activity, and the existence of an unknown ISG15 receptor on DCs that mediates chemotaxis of these cells to the site of infection and IL-1β production is hypothesized (17).

Although the role of ISG15 in antimicrobial activity is unquestioned, here we focused our studies on investigating the function of ISG15 in the generation of immune responses. In breast cancer, it has been demonstrated that free intracellular ISG15 enhanced the expression of major histocompatibility complex class I (MHC-I) and antigen presentation, thus favoring the action of cytotoxic immune cells against the tumor (18). As these results highlight the potential role of ISG15 protein as an adjuvant enhancing immune responses, we decided to analyze this possible function in the context of an HIV/AIDS vaccine candidate following a prime-boost immunization protocol in mice. Our results pointed out a relevant potential role of ISG15 as an adjuvant when it is expressed from a DNA vector in different vaccination protocols. Particularly, when wild-type ISG15-conjugated (ISG15-wt) or mutant unconjugated (ISG15-mut) protein was expressed from a DNA vector in muscle, our results indicated higher infiltration of immune cells after ISG15-mut inoculation than after ISG15-wt

administration. However, both ISG15-wt and ISG15-mut proteins enhance immune cell infiltration in the proximal draining lymph node (DLN). In addition, when we studied the immunostimulatory effect of ISG15-wt or ISG15-mut on the adaptive and memory phases of the immune response, although both ISG15-wt and ISG15-mut act as immune adjuvants by increasing $CD8^+$ T cells, the ISG15-wt protein showed better immunostimulatory activity than ISG15-mut. In correlation with our results, it has been recently described that ISG15 acts as an alarmin in skin by inducing extracellular matrix remodeling, myeloid cell infiltration, and inflammation (19). Hence, our results here revealed the immunomodulatory role of ISG15 and its use in optimized immunization protocols against HIV-1 antigens.

RESULTS

Analysis of wild-type ISG15 and mutated ISG15 expression and ISGylation levels in transfected cells. ISG15-wt contains a C-terminal LRLRGG motif that is necessary for its conjugation to target proteins. To determine whether this conjugation process was involved in ISG15-mediated immunomodulation, we included in this study a mutant ISG15 (ISG15-mut) incapable of conjugation due to a mutated C-terminal LRLRAA motif. To verify the expression of both forms of ISG15 and the absence of ISGylation in the presence of ISG15-mut protein, HEK293T cells were mock transfected or cotransfected with plasmids encoding the ISGylation machinery and DNA-ISG15-wt or DNA-ISG15-mut and analyzed by Western blotting as described in Materials and Methods. The highest level of ISG15 expression was achieved at 48 h posttransfection, presenting high-molecular-weight bands corresponding to ISGylated proteins in cells transfected with DNA-ISG15-wt. As expected, in cells transfected with DNA-ISG15-mut, only the band corresponding to the monomeric form of ISG15 was detected (not shown).

Alarmin effect of ISG15 in muscle. It has been recently published that ISG15 acts as an alarmin when it is expressed from a DNA vector in skin by inducing extracellular matrix remodeling, myeloid cell infiltration, and inflammation (19). Since the intramuscular (i.m.) route is one of the most common vaccine delivery pathways, we decided to evaluate the local effect of ISG15 expression on immune cell infiltration in muscle and proximal draining lymph node (DLN). For this, four groups of animals were intramuscularly inoculated with DNA-ISG15-wt, DNA-ISG15-mut, empty DNA (DNA-φ), or phosphate-buffered saline (PBS). At 48 h postinoculation, total muscle from the site of inoculation and the proximal DLN were excised and processed as described in Materials and Methods, and the different immune cell populations present in muscle and DLN cell suspensions were determined by flow cytometry.

Large amounts of cell infiltration of macrophages, $F480^{high}$ macrophages, neutrophils, NK cells, and DCs were detected in muscle from all groups that received DNA vectors compared with the PBS group, as indicative of DNA sensing by local innate cells; however, in groups where ISG15-wt or ISG15-mut was expressed, the absolute numbers of these populations were significantly higher than those observed in the group that received empty DNA, the infiltration of immune cells being higher in the DNA-ISG15-mut group than in the DNA-ISG15-wt group in muscle (Fig. 1A). A similar behavior in the proximal DLN was observed, with the absolute numbers of macrophages, CD4 and CD8 T cells, and NK and NKT cells being higher in groups receiving DNA-ISG15-wt or DNA-ISG15-mut (Fig. 1B).

Overall, these data indicate that both ISG15-wt and ISG15-mut proteins act as alarmins when expressed from a DNA vector inducing immune cell infiltration in muscle and proximal DLN.

Coadministration of ISG15-wt significantly enhances the magnitude and quality of HIV-1 Env-specific CD8 T cells. We have previously shown that heterologous combination of DNA encoding HIV-1 gp120 protein (DNA-gp120) as a prime followed by modified vaccinia virus Ankara B (MVA-B) vector as a boost is an efficient protocol to induce HIV-1-specific B and T cell immune responses in mice (20–23). Thus, we decided to use this regimen as a model to explore the immunostimulatory effect of

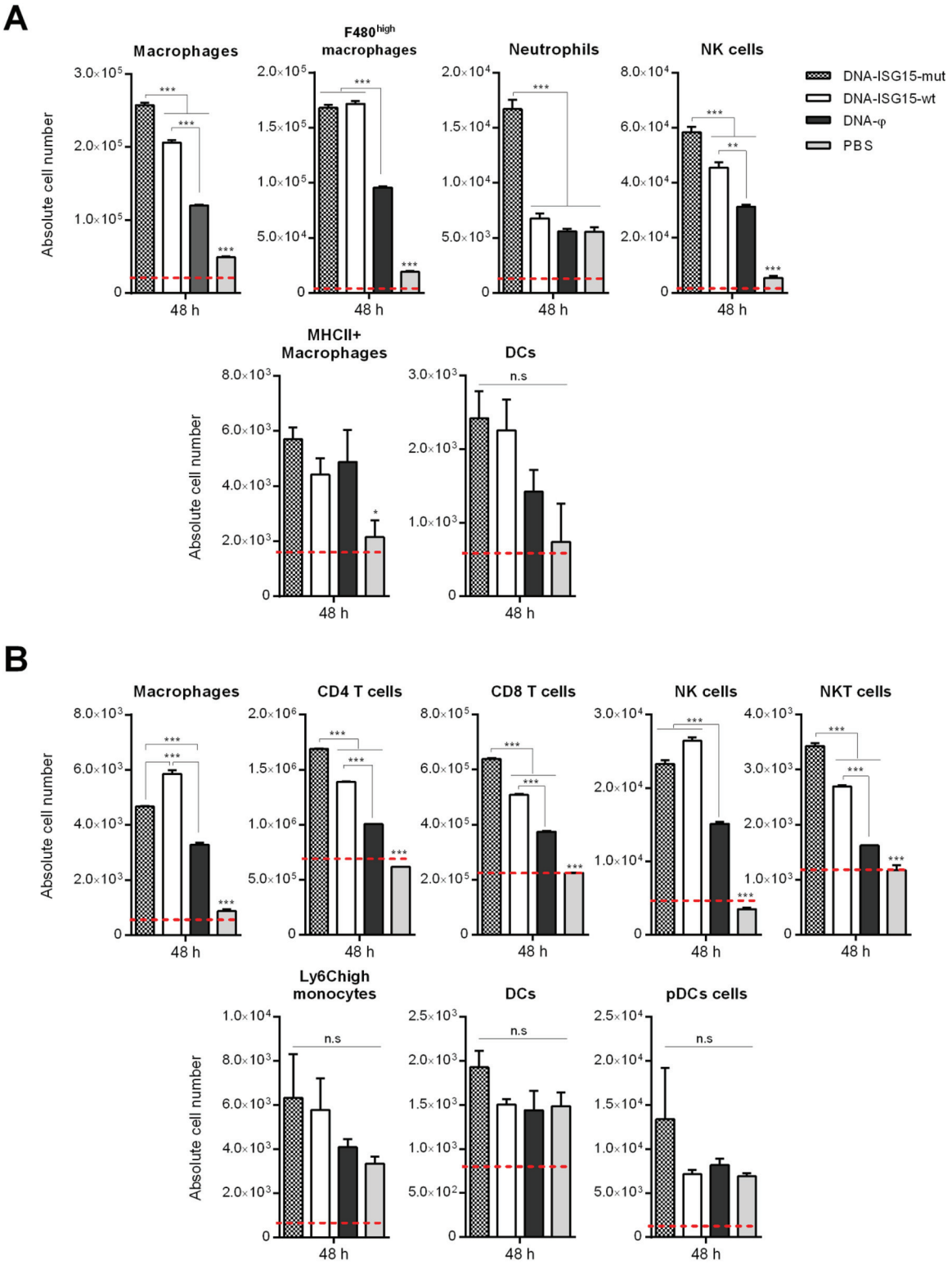

FIG 1 Effect of ISG15 expression on immune cell infiltration. Four groups of animals were inoculated with DNA-ISG15-wt, DNA-ISG15-mut, DNA-φ, or PBS by the intramuscular (i.m.) route. At 48 h postinoculation, total muscle from the site of inoculation and the proximal DLN were excised and processed as described in Materials and Methods, and the different immune cell populations present in muscle (A) and proximal DLN (B) cell suspensions were determined by flow cytometry. The dotted red line indicates the absolute cell numbers of the different cell populations detected in naive mice. n.s., not statistically significant. *, $P < 0.05$; **, $P < 0.005$; ***, $P < 0.001$.

ISG15-wt or ISG15-mut on the adaptive and memory phases of the immune response. For this, four groups of BALB/c mice ($n = 8$) were immunized following the schedule shown in Fig. 2A. At 10 or 53 days postboost, animals were sacrificed to evaluate in spleen the HIV-1- or vaccinia virus (VACV)-specific T cell adaptive or memory immune responses, respectively. The HIV-1 Env-specific T cell responses were evaluated by polychromatic intracellular cytokine staining (ICS) assay after *ex vivo* stimulation of splenocytes with a pool of overlapping peptides that spanned the HIV-1 gp120 protein. The overall magnitude of the HIV-1 Env-specific CD4 and CD8 T cell responses was determined as the percentages of T cells within each subset that produced IFN-γ, IL-2, and/or tumor necrosis factor alpha (TNF-α), whereas the cytotoxic potential was indirectly determined by the expression of the degranulation marker CD107a on the surface of activated cells. The quality of the HIV-1 Env-specific T cells was characterized by the pattern of cytokine production and their cytotoxic potential. At both time points, we also evaluated the humoral response by analyzing the levels of total IgG binding antibodies against the HIV-1 gp120 protein and the anti-gp120 IgG1, IgG2a, and IgG3 subclasses in serum of individual animals by enzyme-linked immunosorbent assay (ELISA).

(i) HIV-1 Env-specific adaptive immune response. As shown in Fig. 2B, and in line with our previous findings (20–23), more than 90% of the overall HIV-1 Env-specific response elicited by the heterologous administration of DNA-gp120 prime–MVA-B boost was mediated by $CD8^+$ T cells. The coadministration of DNA-ISG15-wt or DNA-ISG15-mut with DNA-gp120 in the prime increased even more the prevalence of the HIV-1 Env-specific CD8 T cells over the CD4 T cells (98%), although with differences between groups. In groups receiving DNA-ISG15-wt or DNA-ISG15-mut, the percentages of $CD8^+$ T cells secreting effector cytokines were 5- and 2-fold higher, respectively, than those in the reference group (Fig. 2B, left panel). Similarly, the levels of $CD8^+$ cytotoxic T lymphocytes (CTLs) were 3.4- and 1.5-fold higher in these groups, respectively (Fig. 2B, right panel). When we analyzed the quality of the HIV-1 Env-specific CD8 T cell response, we observed that in all groups more than 70% of the $CD8^+$ T cells exhibited two or more functions; however, DNA-ISG15-wt increased this polyfunctionality profile up to 90% (Fig. 2C). Both DNA-ISG15-wt and DNA-ISG15-mut preferentially increased the $CD8^+$ T cells expressing simultaneously $CD107a^+$ IFN-γ^+ TNF-α, although the magnitude was significantly higher in the DNA-ISG15-wt group.

When we analyzed the HIV-1 Env-specific humoral response at 10 days postboost, we detected high levels of anti-gp120 total IgG binding antibodies in all groups, with medians of endpoint titers ranging from 10^4 to 10^5, except for the negative-control group (DNA-φ/MVA-WT), which showed no reactivity (Fig. 2D, left panel). The anti-gp120 IgG2a/IgG1 or IgG3/IgG1 ratios were similarly low in all groups, evidencing a Th2-associated IgG1 bias response (Fig. 2D, middle and right panels).

Overall, these results indicated that both ISG15-wt and ISG15-mut act as immune adjuvants by increasing the $CD8^+$ T cells; however, the ISG15-wt showed better immunostimulatory activity than ISG15-mut.

(ii) HIV-1 Env-specific memory immune response. At 53 days postboost, we analyzed the magnitude, quality, and memory phenotype of the HIV-1 Env-specific T cell immune responses in the different immunization groups. As in the adaptive phase, the overall long-term HIV-1 Env-specific responses were mediated by CD8 T cells, although the magnitudes of the responses were lower (Fig. 3A). Interestingly, as we observed previously (23, 24), the HIV-1 Env-specific CD8 T cell response in the reference group (DNA-gp120/MVA-B) was minimally reduced, with magnitudes similar to those observed during the adaptive phase. In contrast, in groups where DNA-ISG15-wt or DNA-ISG15-mut was coadministered with DNA-gp120, the overall HIV-1 Env-specific CD8 T cell responses were reduced by 3-fold. Even with this scenario, the magnitude of the HIV-1 Env-specific CD8 T cells was higher when ISG15-wt was expressed. No changes in the polyfunctional profile of the HIV-1 Env-specific CD8 T cells compared with the adaptive response were detected (Fig. 3B).

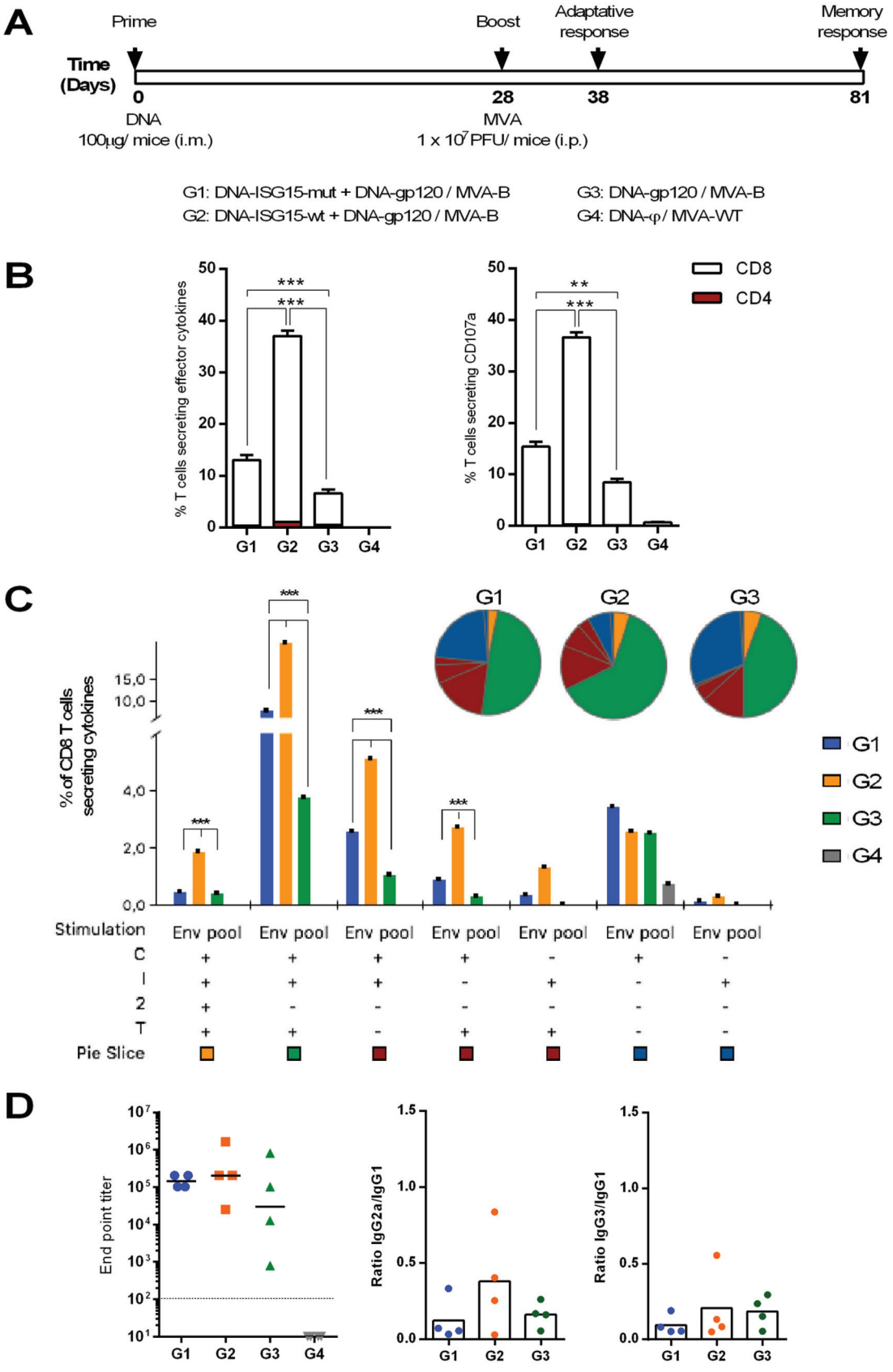

FIG 2 HIV-1 Env-specific cellular and humoral adaptive immune responses elicited in mice after (DNA-ISG15 plus DNA-gp120)

(Continued on next page)

At this time point, we also evaluated the phenotype of the $CD8^+$ T cells by measuring the expression of the CD127 and CD62L surface markers on activated cells. This marker combination allows the classification of the different memory subpopulations in T central memory (TCM; $CD127^+$ $CD62L^+$), T effector memory (TEM; $CD127^+$ $CD62L^-$), and T effector (TE; $CD127^-$ $CD62L^-$) cells. As shown in Fig. 3C, the HIV-1 Env-specific CD8 T cell responses showed a predominant TEM phenotype in all groups.

The long-term humoral HIV-1 gp120-specific response behaved similar to the response observed at the adaptive phase. High levels of anti-gp120 total IgG binding antibodies with medians of endpoint titers of 10^5 (Fig. 3D, left panel) and low anti-gp120 IgG2a/IgG1 or IgG3/IgG1 ratios (Fig. 3D, middle and right panels) were similarly maintained in all groups.

(iii) VACV-specific adaptive and memory T cell immune responses. Since we use a single dose of MVA vector (MVA-B or MVA-WT) as a boost in our immunization groups, we next decided to evaluate the antivector $CD8^+$ T cells. For this, VACV-specific responses were measured by polychromatic ICS assay following the protocol described below, but using the VACV E3 peptide for the *ex vivo* stimulation of the splenocytes from immunized mice. As shown in Fig. 4A, at 10 days postboost, the highest E3-specific CD8 T cell responses were detected in the DNA-φ/MVA-WT control group, indicating that the HIV-1 Env antigen acts as a competitor for the immunodominance of MVA antigens. During the memory phase, the overall magnitude of antivector responses decreased in all groups, but in animals receiving DNA-ISG15-wt, the reduction of the response was lower, and hence the percentages of E3-specific CD8 T cells were similar to those obtained in the DNA-φ/MVA-WT control group (Fig. 4B).

The anti-VACV CD8 T cell responses were highly polyfunctional in all groups during the adaptive and memory phases, with more than 70% of the $CD8^+$ T cells exhibiting two or more functions (Fig. 4C and D). $CD8^+$ T cells expressing simultaneously $CD107a^+$ IFN-γ^+ TNF-α were the most prevalent population. At the memory phase, the VACV-specific CD8 T cell responses showed an effector memory phenotype (TEM; data not shown).

Overall, these results suggest that coadministration of ISG15-wt or ISG15-mut with DNA-gp120 during the prime does not affect the VACV-specific CD8 T cell response induced after MVA boost.

Coadministration of ISG15-wt allows reducing 5-fold the dose of DNA-gp120 without affecting the HIV-1 Env-specific responses. One critical issue in the vaccine field is the antigen dose required for eliciting an optimal immune response. Current clinical trials in which a DNA vector is included normally by the intramuscular (i.m.)

FIG 2 Legend (Continued)
prime followed by MVA-B boost. (A) Immunization schedule. Groups of female BALB/c mice ($n = 8$) received the indicated doses of DNA-based vectors by the i.m. route, and 28 days later, animals were immunized with 1×10^7 PFU of MVA-WT or MVA-B by the intraperitoneal (i.p.) route. At 10 days postboost, 4 mice of each group were sacrificed, spleens were processed for the intracellular cytokine staining (ICS) assay, and sera were harvested for the enzyme-linked immunosorbent assay (ELISA) to measure the cellular and humoral adaptive immune responses against HIV-1 gp120 antigen, respectively. At 53 days postboost, the remaining 4 mice of each group were sacrificed, and spleens and sera were processed as described above to measure the HIV-1 Env-specific cellular and humoral memory immune responses. (B) Magnitude of the HIV-1 Env-specific T cell responses measured at 10 days postboost by ICS assay following *ex vivo* stimulation of splenocytes from immunized mice with the HIV-1 Env clade B consensus peptide pools. The total value in each group represents the sum of the percentages of $CD4^+$ plus $CD8^+$ T cells secreting IL-2, and/or IFN-γ, and/or TNF-α (left panel) or the percentages of $CD4^+$ plus $CD8^+$ T cells expressing CD107a (right panel) against HIV-1 Env clade B consensus peptide pools. All data are background subtracted. The 95% confidence interval (CI) is represented. **, $P < 0.005$; ***, $P < 0.001$. (C) Polyfunctional profile of the HIV-1 Env-specific CD8 T cell responses in the different immunization groups. The seven positive combinations of the responses are indicated on the *x* axis, while the percentages of the functionally different cell populations within the total CD8 T cells are represented on the *y* axis. Specific responses are grouped and color coded based on the number of functions. Abbreviations: C, CD107a; I, IFN-γ; 2, IL-2; T, TNF-α. ***, $P < 0.001$. (D, left panel) Levels of HIV-1 gp120 Bx08-specific total IgG binding antibodies measured in the sera from individual immunized mice at 10 days postboost by ELISA. The different colored shapes represent the antibody titers for each mouse defined as the last serum dilution that gave three times the mean optical density at 450 nm (OD_{450}) of the control group (endpoint titer): the solid horizontal line indicates the mean antibody titer for each group, and the dotted horizontal line represents the detection limit of the assay. (Middle and right panels) Levels of HIV-1 gp120 Bx08-specific IgG1, IgG2a, and IgG3 binding antibodies were measured in individual sera from immunized mice at 10 days postboost as the OD_{450} at a serum dilution of 1:25,600 by ELISA, and ratios of IgG2a to IgG1 (middle) and IgG3 to IgG1 (right) are represented. The different colored circles represent the antibody ratios for each mouse, and the open columns indicate the mean antibody ratios for each group.

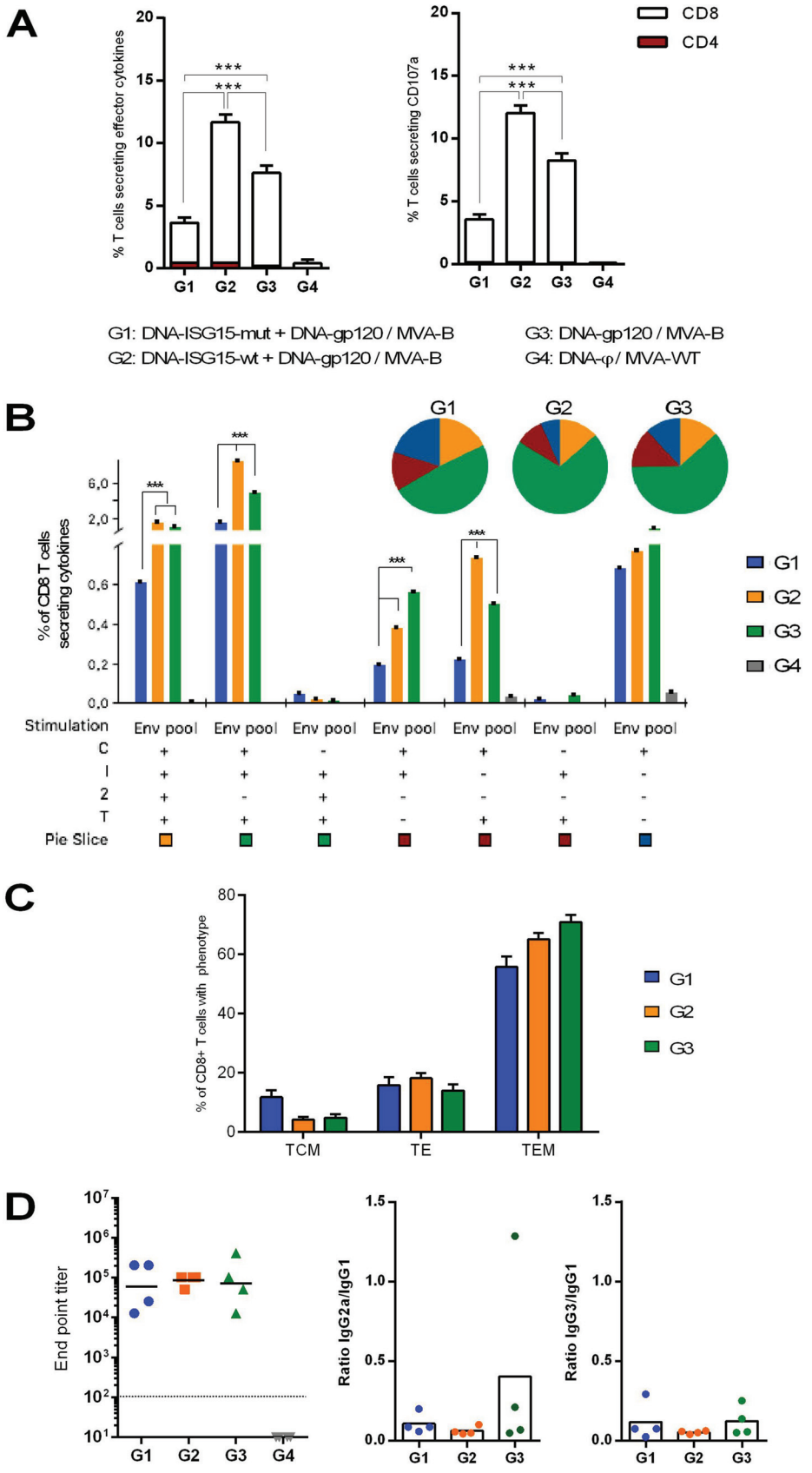

FIG 3 HIV-1 Env-specific cellular and humoral memory immune responses elicited in mice after (DNA-ISG15 plus DNA-gp120) prime followed by MVA-B boost. (A) Magnitude of the HIV-1 Env-specific T cell

(Continued on next page)

route use between 1 and 4 mg of DNA/dose (https://aidsinfo.nih.gov). In this context, adjuvants can be used to increase the immunogenicity elicited by heterologous antigens and, therefore, to reduce the antigen dose needed. Thus, once we had demonstrated the immunostimulatory properties of ISG15-wt on the HIV-1 Env-specific CD8 T cell responses, we next decided to evaluate whether this response could be modulated by the coadministration of ISG15-wt with decreasing doses of DNA-gp120. For this purpose, five groups of animals ($n = 4$) were immunized as shown in Fig. 5A. We used a total DNA amount of 100 μg for prime. In the different test groups, we combined 50 μg of DNA-ISG15-wt with decreasing amounts of DNA-gp120 (50, 25, and 10 μg) to compare with the reference group, which received 50 μg of DNA-gp120 plus 50 μg of DNA-φ. At 10 days postboost, the overall HIV-1 Env-specific CD4 and CD8 T cell responses were determined as previously described. As shown in Fig. 5B, and consistent with our previous results (Fig. 2B), the overall HIV-1 Env-specific T cell responses were mainly mediated by CD8 T cells. The coadministration of DNA-ISG15-wt allows reducing 5-fold the amount of DNA-gp120 necessary to induce similar responses to the reference group (DNA-gp120/MVA-B). Interestingly, in the group where ISG15-wt was coadministered with half the amount (25 μg) of DNA-gp120, the total percentages of effector cytokines and CD8 CTL cells were significantly higher than in the reference group and similar to those in the group receiving DNA-ISG15-wt plus 50 μg of DNA-gp120. The polyfunctional profiles of the $CD8^+$ T cells were similar in all groups (Fig. 5C), with the population simultaneously expressing $CD107a^+$ IFN-γ^+ TNF-α being the most induced. Additionally, no changes in the levels of anti-gp120 total IgG binding antibodies were detected when decreasing doses of DNA were assayed (Fig. 5D).

Overall, these results confirm the immune adjuvant properties of ISG15-wt when decreasing amounts of heterologous DNA-gp120 are used, without affecting the potency and the quality of the HIV-1 Env-specific immune responses.

DISCUSSION

Vaccines are one of the most cost-effective medical treatments in modern civilization, but the development of an effective vaccine against HIV/AIDS has proven to be one of the greatest complex scientific challenges. Despite the progress that has been made in the field, currently no vaccine candidate has improved the 31.2% efficacy demonstrated in the RV144 trial (25). Overcoming this challenging task requires a multidisciplinary approach, which includes the design of novel immunogens, the development of optimized adjuvants, the testing of different vaccination routes/schedules, and the generation of novel delivery vectors, with the aim to induce effective HIV-1-specific T and B cell immune responses. Finding new adjuvants is, therefore, one of the components that should be optimized for the development of an effective HIV-1 vaccine. Compared with traditional adjuvants, such as alum, a novel adjuvant in the HIV-1 field should preferentially trigger a durable and potent memory

FIG 3 Legend (Continued)
responses measured at 53 days postboost by ICS assay following *ex vivo* stimulation of splenocytes from immunized mice with the HIV-1 Env clade B consensus peptide pools. The total value in each group represents the sum of the percentages of $CD4^+$ plus $CD8^+$ T cells secreting IL-2, and/or IFN-γ, and/or TNF-α (left panel) or the percentages of $CD4^+$ plus $CD8^+$ T cells expressing CD107a (right panel) against HIV-1 Env clade B consensus peptide pools. All data are background subtracted. The 95% CI is represented. ***, $P < 0.001$. (B) Polyfunctional profile of the HIV-1 Env-specific CD8 T cell responses in the different immunization groups. The seven positive combinations of the responses are indicated on the *x* axis, while the percentages of the functionally different cell populations within the total CD8 T cells are represented on the *y* axis. Specific responses are grouped and color coded based on the number of functions. Abbreviations: C, CD107a; I, IFN-γ; 2, IL-2; T, TNF-α. ***, $P < 0.001$. (C) Phenotypic profile of the memory HIV-1 Env-specific CD8 T cells. The phenotype of the vaccine-induced memory responses was determined based on expression of the CD127 and CD62L surface markers on activated cells as follows: T central memory (TCM; $CD127^+$ $CD62L^+$), T effector memory (TEM; $CD127^+$ $CD62L^-$), and T effector (TE; $CD127^-$ $CD62L^-$) cells. (D, left panel) Levels of HIV-1 gp120 Bx08-specific total IgG binding antibodies measured in the sera from individual immunized mice at 53 days postboost by ELISA. (Middle and right panels) Levels of HIV-1 gp120 Bx08-specific IgG1, IgG2a, and IgG3 binding antibodies were measured in individual sera from immunized mice at 53 days postboost as the OD_{450} at a serum dilution of 1:25,600 by ELISA, and ratios of IgG2a to IgG1 (middle) and IgG3 to IgG1 (right) are represented.

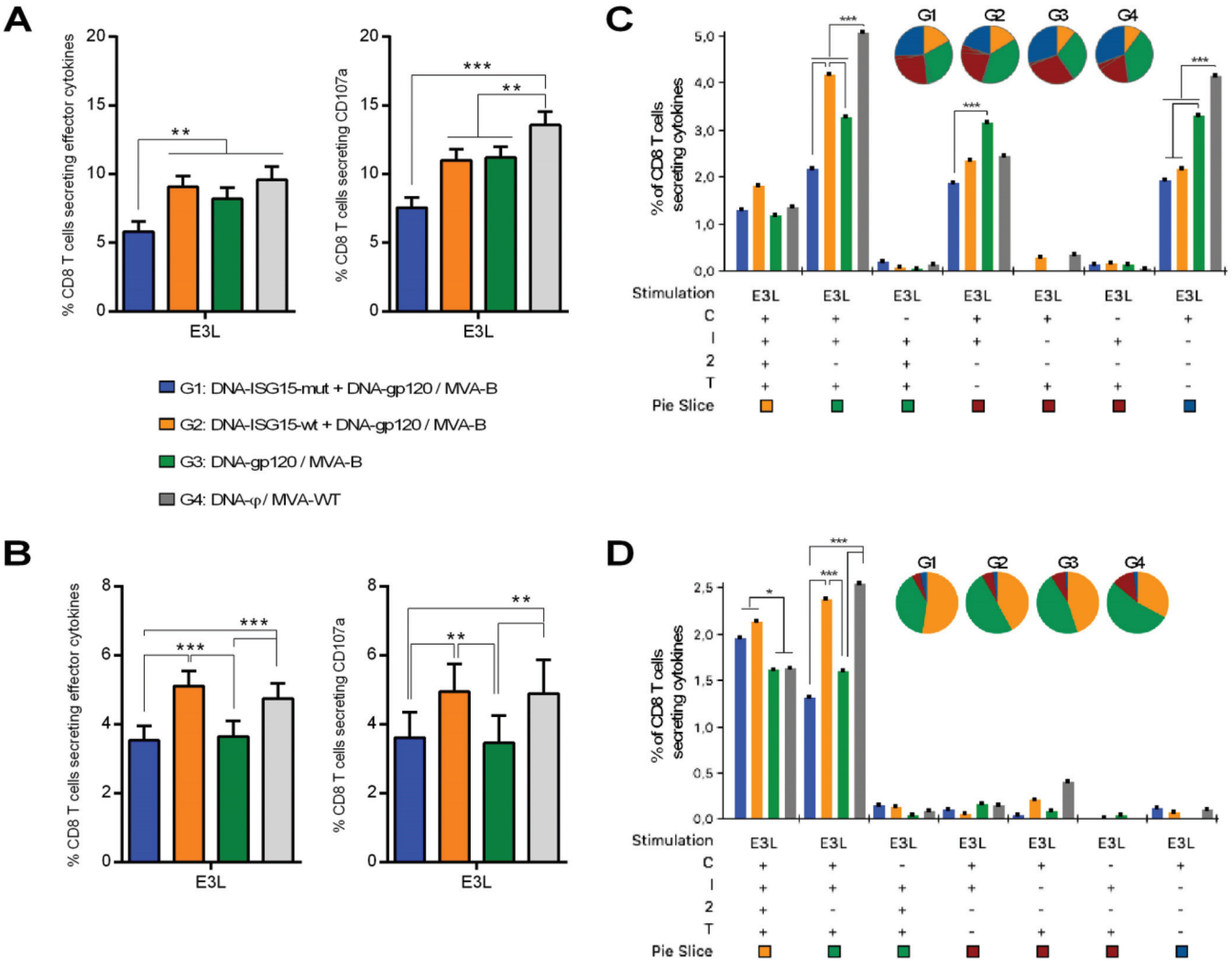

FIG 4 VACV E3-specific CD8 T cells elicited in mice after (DNA-ISG15 plus DNA-gp120) prime followed by MVA-B boost at adaptive and memory phases of the immune response. (A and B) Magnitude of the VACV E3-specific CD8 T cell responses measured at 10 (A) or 53 (B) days postboost by ICS assay following *ex vivo* stimulation of splenocytes from immunized mice with the VACV E3 peptide. The total value in each group represents the sum of the percentages of $CD8^+$ T cells secreting IL-2, and/or IFN-γ, and/or TNF-α (left panels) or the percentages of $CD8^+$ T cells expressing CD107a (right panels) against VACV E3 peptide. All data are background subtracted. The 95% CI is represented. **, $P < 0.005$; ***, $P < 0.001$. (C and D) Polyfunctional profiles of the VACV E3-specific CD8 T cell response in the different immunization groups at 10 (C) or 53 (D) days postboost. The seven positive combinations of the responses are indicated on the *x* axis, while the percentages of the functionally different cell populations within the total CD8 T cells are represented on the *y* axis. Specific responses are grouped and color coded based on the number of functions. Abbreviations: C, CD107a; I, IFN-γ; 2, IL-2; T, TNF-α. *, $P < 0.05$; ***, $P < 0.001$.

response from B cells, CD8 T cells, and/or NK cells but avoid overstimulation of HIV-1-susceptible CD4 T cells (26). In this context, we explored here the immunomodulatory properties of ISG15 when it is expressed by a DNA vector in a setting of a heterologous DNA-gp120 prime–MVA-B boost immunization regimen.

ISG15 is a ubiquitin-like protein expressed mainly in monocytes, lymphocytes, and neutrophils, as well as in DCs, NK cells, epithelial tissue-derived cell lines, fibroblasts, and several tumor cells (1, 13, 27, 28). Over the last decade, a detailed study of the functions of ISG15 in response to pathogen invasion has been performed. The antiviral activity of ISG15 is mostly associated with its canonical function as an intracellular posttranslational modifier (29). However, other functions independent of the conjugation activity, such as intracellular attenuation of IFN-α/β signaling (12) or as an extracellular cytokine, have been recently reported (14). Identification of the relationships between the extracellular and the intracellular conjugation-dependent and -independent functions of ISG15 is likely to reveal critical connections among innate

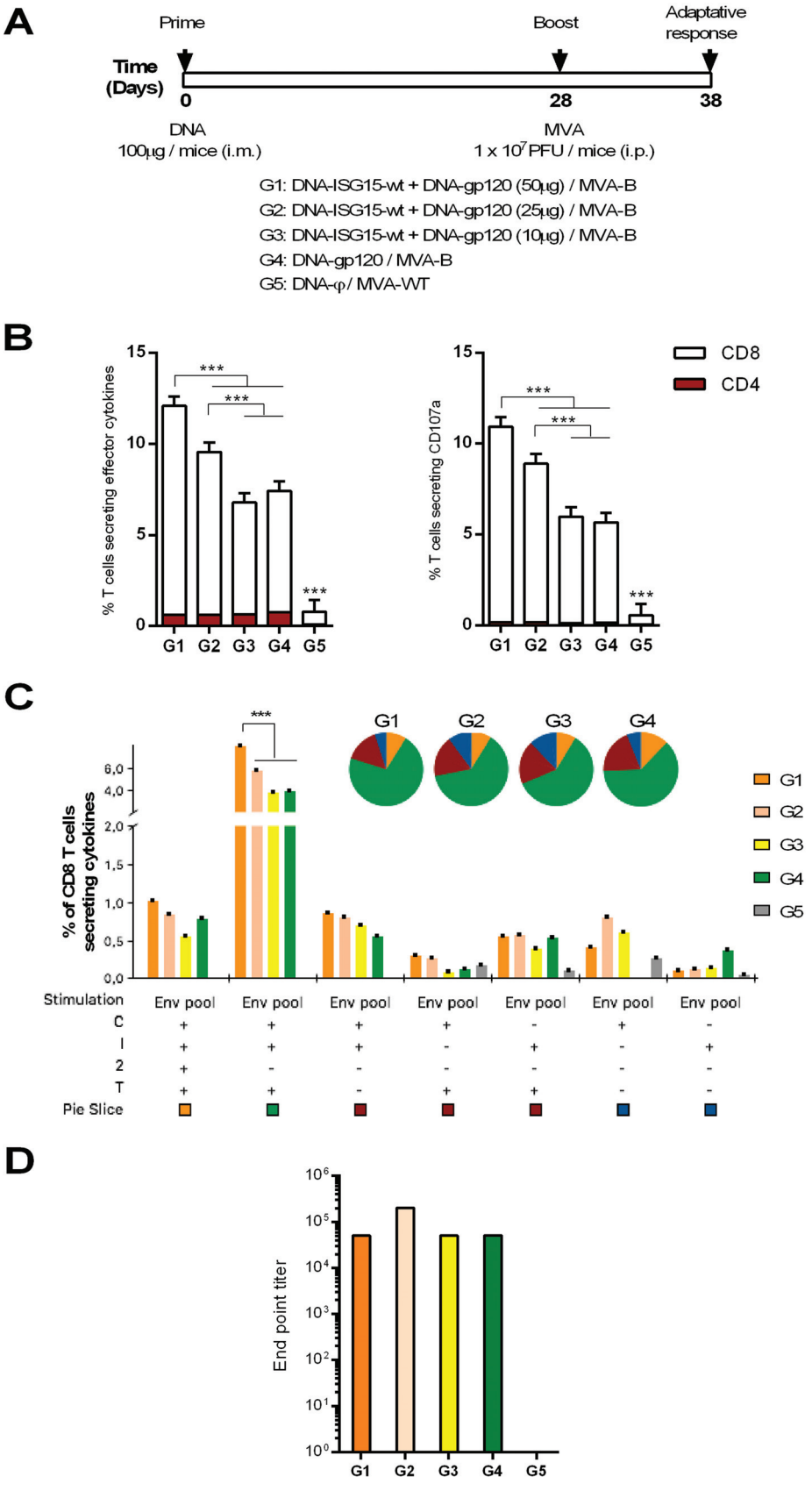

FIG 5 HIV-1 Env-specific cellular and humoral adaptive immune responses elicited in mice after the administration of DNA-ISG15-wt with decreasing amounts of DNA-gp120 in the prime followed by the MVA-B

(Continued on next page)

immune responses and provide opportunities for modulation of responses to infectious diseases (30).

The immunomodulatory role of extracellular ISG15 was initially defined based on cell culture experiments, which evidenced that ISG15 works in synergy with IL-12 to stimulate the release of IFN-γ from peripheral blood mononuclear cells (PBMCs), most notably from NK cells and, to a lesser degree, from T cells (17). Recently, the discovery of LFA-1 as the ISG15 cell surface receptor and the downstream signaling events leading to IFN-γ secretion extended our knowledge on the putative cytokine function of free ISG15 (16). However, only three studies have assayed the immune adjuvant role of ISG15 *in vivo* against cancer (18, 19, 31). In the context of breast cancer, it has been established that vaccination against ISG15 results in major CD8-mediated diminutions in both primary and metastatic mammary tumor burdens (31). In the other studies, using a human papillomavirus (HPV)-associated tumor murine therapeutic model, these authors demonstrated that ISG15 acts as an immunoadjuvant, independently of conjugation. Recently, Iglesias-Guimarais et al. demonstrated that extracellular ISG15 is an alarmin that promoted the vaccine-specific CTL response by enhancing $CD8^+$ T cells mostly via NK cells (19). These authors, using an elegant deep-sequencing approach from the skin area after vaccination, concluded that at the molecular level, ISG15 induces tissue alert, represented by upregulation of metalloproteases and collagens, suggesting the remodeling of the extracellular matrix. In addition, they found several members of myeloid cell infiltration and inflammation categories (19).

Here, we observed that the intramuscular delivery of DNA vectors expressing ISG15-wt or ISG15-mut proteins in mice induced enhanced immune cell infiltration in muscle and proximal DLN. This innate activation at the inoculation site seemed to impact the HIV-1 Env-specific adaptive and memory CD8 T cell responses when DNA-ISG15-wt or DNA-ISG15-mut was coadministered with DNA-gp120 in the prime, since enhanced magnitude of effector $CD8^+$ T cells with cytotoxic capacity and polyfunctional profile were detected in these groups. Regarding the migratory capacity of macrophages stimulated after intramuscular plasmid inoculation, our results do not evidence any relevance of ISGylation, as our colleagues have previously reported in the papillomavirus system in the dermis. However, in contrast to previous findings, we observed that ISG15-wt exhibits better immunostimulatory activity than ISG15-mut, indicating that in addition to the free ISG15 or intracellular conjugation-independent functions, the intracellular ISGylation also plays an important role in the connection between innate and adaptive immunities.

The discrepancy between our results and previous *in vivo* studies could be explained by the immunization regimen used, which involves different doses of ISG15 adjuvant. Villareal et al. immunized the animals with a homologous DNA/DNA regimen using intramuscular/electroporation delivery at 2-week intervals, while Iglesias-Guimarais et al. used shorter time intervals (3 days) to deliver 3 doses of DNA vectors by intraepidermal tattoo. In both studies,

FIG 5 Legend (Continued)
boost. (A) Immunization schedule. Groups of female BALB/c mice ($n = 4$) received the indicated doses of DNA-based vectors by the i.m. route, and 28 days later, animals were immunized with 1×10^7 PFU of MVA-WT or MVA-B by the i.p. route. At 10 days postboost, animals were sacrificed, spleens were processed for the ICS assay, and sera were harvested for ELISA to measure the cellular and humoral adaptive immune responses against HIV-1 gp120 antigen, respectively. (B) Magnitude of the HIV-1 Env-specific T cell responses measured at 10 days postboost by the ICS assay following *ex vivo* stimulation of splenocytes from immunized mice with the HIV-1 Env clade B consensus peptide pools. The total value in each group represents the sum of the percentages of $CD4^+$ plus $CD8^+$ T cells secreting IL-2, and/or IFN-γ, and/or TNF-α (left panel) or the percentages of $CD4^+$ plus $CD8^+$ T cells expressing CD107a (right panel) against HIV-1 Env clade B consensus peptide pools. All data are background subtracted. The 95% CI is represented. ***, $P < 0.001$. (C) Polyfunctional profile of the HIV-1 Env-specific CD8 T cell responses in the different immunization groups. The seven positive combinations of the responses are indicated on the *x* axis, while the percentages of the functionally different cell populations within the total CD8 T cells are represented on the *y* axis. Specific responses are grouped and color coded based on the number of functions. Abbreviations: C, CD107a; I, IFN-γ; 2, IL-2; T, TNF-α. ***, $P < 0.001$. (D) Levels of HIV-1 gp120 Bx08-specific total IgG binding antibodies measured in pooled sera from immunized mice at 10 days postboost by ELISA. The endpoint titer is defined as the last serum dilution that gave three times the mean optical density at 450 nm (OD_{450}) of the control group.

the ISG15 proteins were codelivered with the vaccine antigen at least two times. Here, we immunized the animals by intramuscular and intraperitoneal routes using a heterologous DNA (i.m.)-MVA (i.p.) regimen at 4-week intervals, and hence the animals received the ISG15 adjuvant only once in the prime. Another explanation for the discrepancies observed could be attributable to vaccination system. The aim of the present study was the optimization of an effective vaccine against HIV/AIDS, using DNA-gp120 as antigen delivery vector administered in the prime. It has been reported that ISG15 protein is dramatically increased in transgenic mice overexpressing HIV-1 gp120 protein (32). Specifically, ISG15 and its conjugates were remarkably elevated in the cortex and hippocampus of gp120 mice (32). These results may indicate a difference in the ISG15 and ISGylation levels after gp120 overexpression that may vary the results with respect to the aforementioned tumor models.

Taking into consideration all the above data, we hypothesized that in the context of an HIV/AIDS vaccine candidate following a prime-boost immunization protocol in mice, in addition to the secreted unconjugated form of ISG15, another source of extracellular ISG15 conjugates might be produced intracellularly. ISGylated proteins might be transported to the surface of transfected cells or released due to cell death. These different sources of extracellular ISG15 conjugates could potentially engage LFA-1 on NK cells and contribute to the enhanced CD8 T cell responses that we observed in animals receiving DNA-ISG15-wt. In this context, the maintenance of the potency and quality of the HIV-1 Env-specific immune responses in the presence of ISG15-wt when decreasing amounts of heterologous DNA-gp120 were used is a finding of special relevance for the vaccine development field.

Overall, this study reveals the immunomodulatory properties of either ISG15-wt or ISG15-mut proteins when expressed by a DNA vector, conferring immune potency to an HIV-1 vaccine candidate, with a possible role for ISGylation in the connection between innate and adaptive immunities. Hence, the DNA-ISG15 vector could be used as a promising CD8 T cell-driven vaccine adjuvant for the modulation of specific immune responses to HIV-1 or other vaccine candidates to enhance control of infectious diseases.

MATERIALS AND METHODS

Cells and viruses. HEK293T cells (a highly transfectable cell line derivative of human embryonic kidney 293 cells; ATCC catalog no. CRL-3216), primary chicken embryo fibroblast (CEF) cells (obtained from pathogen-free 11-day-old eggs; MSD, Salamanca, Spain), and DF-1 cells (a spontaneously transformed CEF cell line; ATCC catalog no. CRL-12203) were cultured in Dulbecco's modified Eaglés medium (DMEM; Invitrogen Gibco, NY, USA) supplemented with 2 mM L-glutamine (Merck, Kenilworth, NJ, USA), 100 U/ml penicillin–100 μg/ml streptomycin (Sigma-Aldrich, St. Louis, MO, USA), 0.1 mM nonessential amino acids (Sigma-Aldrich), 0.5 μg/ml amphotericin B (Fungizone; Gibco-Life Technologies, Waltham, MA, USA), and 10% heat-inactivated fetal calf serum (FCS; Sigma-Aldrich) and maintained at 37°C in a humidified air incubator with 5% CO_2 atmosphere.

The poxviruses used in this work included the attenuated wild-type modified vaccinia virus Ankara (MVA-WT) obtained from the Ankara strain after 586 serial passages in CEF cells (provided by Gerd Sutter, Ludwig-Maximilians-University of Munich, Munich, Germany) and the MVA-B recombinant virus, which simultaneously expresses the full-length HIV-1 Gag-Pol-Nef (GPN) fusion protein as an intracellular product and the monomeric gp120 as a cell-released product of clade B from the viral thymidine kinase (TK) locus (*J2R* gene) (33). Viruses were grown in CEF cells with DMEM–2% FCS and purified through two 36% (wt/vol) sucrose cushions. The virus titers were determined by immunostaining plaque assay in monolayers of DF-1 cells, as previously described (34).

DNA vectors. DNA vectors used in this work included the plasmids pCAGGS-φ (DNA-φ), pCAGGS-GFP (encoding GFP reporter gene), pCAGGS-ISG15-GG (encoding wild-type murine ISG15 [DNA-ISG15-wt]), pCAGGS-ISG15-AA (encoding the no-ISGylable form of murine ISG15 [DNA-ISG15-mut]), pCMV-φ, and pCMV-gp120 Bx08 (encoding the HIV-1 clade B Bx08 gp120 protein [DNA-gp120]). pCAGGS mammalian expression vectors encoding murine ISG15 (-wt or -mut) fused to the V5 tag at its N-terminal end were kindly provided by Adolfo García-Sastre (Mount Sinai Hospital, New York, NY, USA). Plasmid pCMV-gp120 Bx08 has been previously described (33). Plasmids were purified using the EndoFree Plasmid Mega kit (Qiagen, Hilden, Germany) and diluted for injection in endotoxin-free phosphate-buffered saline (PBS).

Transfection assays. To determine the correct expression of murine ISG15-wt or ISG15-mut, monolayers of HEK293T cells grown in 24-well plates at 70 to 80% confluence were cotransfected with 200 ng of each plasmid encoding murine E1, E2, and E3 ligases together with 400 ng of pCAGGS-ISG15-AA or pCAGGS-ISG15-GG using TransIT-LT1 transfection reagent (Mirus Bio, LLC, Madison, WI, USA) according to the manufacturer´s recommendations.

Western blotting. At 24 to 48 h posttransfection, cells were harvested and lysed in 1× Laemmli buffer. Cell extracts were then fractionated by 12% SDS-PAGE and analyzed by Western blotting using mouse monoclonal anti-V5 Tag antibody (1:5,000; Thermo Fisher Scientific, Carlsbad, CA, USA) to evaluate

ISGylation or ISG15 expression. The mouse monoclonal anti-β-actin 8H10D10 antibody (1:1,000; Cell Signaling, Danvers, MA, USA) was used as a loading control. Horseradish peroxidase (HRP)-conjugated goat anti-mouse antibody (1:10,000; Sigma-Aldrich) was used as conjugated secondary antibody. Immune complexes were detected by the enhanced chemiluminescence system using Clarity Western ECL substrate (Bio-Rad, CA, USA) and imaged via the ChemiDoc system (Bio-Rad).

Mouse immunizations. Animal experimental protocols were approved by the Ethical Committee of Animal Experimentation (CEEA) of Centro Nacional de Biotecnología (CNB-CSIC; Madrid, Spain) according to Spanish National Royal Decree RD 53/2013, Spanish National Law 32/2007 on animal welfare, exploitation, transport, and sacrifice, and International EU Guidelines 2010/63/UE on protection of animals used for experimentation and other scientific purposes (permit no. PROEX 281/16). Female BALB/c mice (6 to 8 weeks old) used for immunogenicity assays were purchased from Envigo Laboratories (Indianapolis, IN, USA) and kept in the animal facility of the CNB (Madrid, Spain).

To evaluate the local effect of ISG15 expression on immune cell infiltration in muscle and proximal draining lymph node (DLN), three groups of BALB/c mice ($n = 4$) were immunized with 100 μg of a DNA mixture containing 50 μg of DNA-ISG15-mut, DNA-ISG15-wt, or DNA-φ and 50 μg of pCAGGS-GFP by the intramuscular (i.m.) route (groups 1 to 3). PBS-treated animals were used as the control (group 4). At 48 h postinoculation, animals were sacrificed, and total muscle from the site of inoculation and the proximal DLN were excised and processed for the analysis of different immune cell populations by flow cytometry.

To characterize the immunostimulatory effect of ISG15-wt or ISG15-mut on the HIV-1 Env-specific adaptive and memory phases of the immune response, three groups of BALB/c mice ($n = 8$) were immunized with 100 μg of a DNA mixture containing 50 μg of DNA-ISG15-mut, DNA-ISG15-wt, or DNA-φ and 50 μg of DNA-gp120 by the i.m. route (groups 1 to 3). Group 4 received 100 μg of DNA-φ. Four weeks later, mice were immunized with 1×10^7 PFU of MVA-B (groups 1 to 3) or MVA-WT (group 4) by the intraperitoneal (i.p.) route. At 10 and 53 days postboost, four animals of each group were sacrificed, spleens were processed for the intracellular cytokine staining (ICS) assay, and sera were harvested for the enzyme-linked immunosorbent assay (ELISA) to determine both cellular and humoral HIV-1 Env-specific adaptive and memory immune responses, respectively.

To evaluate whether the HIV-1 Env-specific response could be modulated by the coadministration of ISG15-wt with decreasing doses of DNA-gp120, groups of BALB/c mice ($n = 4$) were immunized with 100 μg of a DNA mixture containing 50 μg of DNA-ISG15-wt and decreasing doses (50, 25, or 10 μg) of DNA-gp120 (completed up to 50 μg with pCMV-φ) by the i.m. route (groups 1 to 3). Group 4 received 50 μg of DNA-φ plus 50 μg of DNA-gp120, and group 5 was inoculated with 50 μg of DNA-φ plus 50 μg of pCMV-φ. Four weeks later, mice were immunized with 1×10^7 PFU of MVA-B (groups 1 to 4) or MVA-WT (group 5) by the i.p. route. At 10 days postboost, animals were sacrificed, spleens were processed for the ICS assay, and sera were harvested for ELISA to determine both cellular and humoral HIV-1 Env-specific adaptive immune responses, respectively.

Processing of murine muscle for the analysis of immune cell infiltration by flow cytometry. Muscle tissue from the injection site was obtained during necropsy at 48 h postinoculation. For this procedure, total muscle from the site of inoculation was dissected with a scalpel, and pooled muscle tissues of each group were placed in complete RPMI 1640 medium (Sigma-Aldrich; 2 mM L-glutamine, 100 U/ml of penicillin–100 μg/ml of streptomycin, 10 mM HEPES, and 0.01 mM β-mercaptoethanol) with 10% FCS and stored on ice until processing. For this, muscle pieces were drained, transferred to a petri dish containing 8 ml dissociation solution (complete RPMI medium–5% FCS supplemented with 0.1 mg/ml DNase I and 1.6 mg/ml collagenase VIII [both from Sigma-Aldrich]), and cut into smaller pieces with tweezers and a scalpel (mechanical dissociation). Enzymatic digestion was then performed by transferring the muscle tissue samples in dissociation solution to a 50-ml Falcon tube and incubating for 30 min at 37°C with vortexing every 10 min. The digested pieces of muscle were then filtered through 40-μm-pore cell strainers (BD Bioscience, San Jose, CA, USA), washed twice with 1× PBS–2% FCS by centrifugation for 5 min at 1,500 rpm, resuspended in 1× PBS–2% FCS, and finally seeded on a 96-well plate according to the number of flow cytometry staining panels.

Peptides. The HIV-1 clade B consensus peptide pools used in this work include Env-1 (63 peptides) and Env-2 (61 peptides). They were provided by the National Institutes of Health (NIH) AIDS Research and Reference Reagent Program (Germantown, MD, USA) and covered the HIV-1 clade B Env protein included in DNA-gp120 and MVA-B vectors as consecutive 15-mers overlapping by 11 amino acids. The VACV $E3_{140\text{-}148}$ peptide (sequence VGPSNSPTF; CNB-CSIC Proteomics Service, Madrid, Spain), previously described as an immunodominant epitope in BALB/c mice (35), was used to determine VACV-specific CD8 T cell responses.

Analysis of immune cell infiltration by flow cytometry. To analyze the local effect of ISG15 expression on immune cell infiltration in muscle and proximal DLN, 2×10^6 cells from muscle or DLN seeded on 96-well plates in 1× PBS–2% FCS (myocytes) or complete RPMI medium–10% FCS (lymphocytes from DLN) were centrifuged, washed once with fluorescence-activated cell sorter (FACS) buffer (1× PBS–2 mM EDTA–1% bovine serum albumin [BSA]), and incubated with the LIVE/DEAD fixable violet or Read Dead Cell stain kits (Invitrogen) for 30 min at 4°C in the dark. After washing twice with FACS buffer and blocking Fc receptors by incubation with anti-CD16/CD32 antibody (BD Biosciences, San Jose, CA, USA) for 15 min at 4°C in the dark, cells were incubated for 20 min at 4°C in the dark with fluorochrome-conjugated surface antibodies for the identification of different immune cell populations (macrophages, neutrophils, NK cells, CD4 and CD8 T cells, monocytes, and DCs) as follows. (i) For staining 1, MHC-II–fluorescein isothiocyanate (FITC), Ly6G-phycoerythrin (PE), CD19-PE, CD3-PE, SinglecF-PE, MHC-II (IA/IE)-biotin (Biot)/avidin (Av)-PECF594, Ly6C-Biot/Av-peridinin chlorophyll protein (PerCP), CD86-PE-Cy5, F480-PE-Cy7, CD8-PE-Cy7, CD64-allophycocyanin (APC), CD11c-APC, CD11b-Alexa Fluor 700, CD3-APC-eFluor

780, CD19-APC-Cy7, CD11c-APC-Cy7, CD45-PB, B220-BV510, and CD45-BV570 were used. (ii) For staining 2, γδTCRT-PE, CD3-PECF594, CD19-SPRD, Gr-1–PerCP–Cy5.5, CD8-PE-Cy7, NKG2D-APC, CD49b-Alexa 700, CD4-APC-Cy7, and CD45-BV570 were used. All antibodies for staining 1 and staining 2 were from BD Biosciences.

Analysis of the cellular immune response by intracellular cytokine staining assay. To analyze the magnitude and phenotype of the HIV-1 Env- or VACV-specific T cell immune responses, 2×10^6 splenocytes (erythrocyte depleted) seeded on 96-well plates were stimulated *ex vivo* for 6 h in complete RPMI medium with 10% FCS, anti-CD107a-FITC (BD Biosciences), 1 μl/ml Golgiplug (BD Biosciences), 1× monensin (Invitrogen), and 5 μg/ml of the HIV-1 Env clade B consensus peptide pools (Env-1 plus Env-2) or 10 μg/ml of VACV E3 peptide. After stimulation, splenocytes from immunized mice were stained for surface markers, fixed/permeabilized (Cytofix/Cytoperm kit; BD Biosciences), and stained intracellularly. The following fluorochrome-conjugated antibodies were used: IL-2–APC, IFN-γ–PECy7, and TNF-α–PE for functional analyses and CD3-PECF594, CD4-APC-Cy7, CD8-V500, CD127-PerCP-Cy5.5, and CD62L-Alexa 700 for phenotypic analyses (all from BD Biosciences). The dead cells were excluded using the LIVE/DEAD fixable violet dead cell stain kit (Invitrogen).

Cells for flow cytometry analysis were acquired in a Gallios flow cytometer (Beckman Coulter, Brea, CA, USA), and data analyses were carried out using FlowJo software (version 10.4.2; Tree Star, Ashland, OR, USA). Lymphocyte-gated events ranged between 10^5 and 5×10^5. After gating, Boolean combinations of single functional gates were generated to quantify the frequency of each response based on all the possible combinations of cytokine expression or differentiation markers. Background responses in the unstimulated controls (RPMI) were subtracted from those obtained in stimulated samples for each specific functional combination.

HIV-1 Env-specific antibody measurement by enzyme-linked immunosorbent assay. Antibody binding to HIV-1 gp120 Bx08 protein in serum was determined by ELISA as previously reported (36). Briefly, individual or pooled sera from immunized mice were 2-fold serially diluted in duplicates and incubated with 2 μg/ml of recombinant HIV-1 gp120 Bx08 purified protein (kindly provided by Suresh Chithathur). Levels of HIV-1 Env-specific total IgG binding antibodies or IgG1, IgG2a, or IgG3 subclasses were established as the last serum dilution that gave 3 times the mean optical density at 450 nm (OD_{450}) of the control group (endpoint titer) or as the OD_{450} at a serum dilution of 1:25,600, respectively.

Data analysis and statistics. For the analysis of ICS data, a statistical approach that adjusts the values for the nonstimulated controls (RPMI) and calculates the confidence intervals and *P* values was used (37). Only antigen responses significantly higher than those of the corresponding RPMI samples are represented. When indicated, the values represented are background subtracted. For the analysis of ELISA data, a one-way analysis of variance (ANOVA) followed by Tukey's honest significant difference criterion was carried out.

ACKNOWLEDGMENTS

We thank Ana Isabel Morato, Cristina Sánchez-Corzo, and Victoria Jiménez for expert technical assistance.

This project was supported by the Spanish Ministerio de Economía, Industria y Competitividad and FEDER/FSE (SAF2017-88089-R to S.G. and M.E.). Michela Falqui received a Formación de Personal Investigador Ph.D. fellowship from the Spanish Ministry of Health and Education.

We declare no conflicts of interest.

C.E.G., B.P., J.G.-A., M.B., M.E., and S.G. conceived and designed the experiments. C.E.G., B.P., J.G.-A., M.B., M.F., and M.Q. performed the experiments. C.E.G., B.P., J.G.-A., C.O.S.S., M.B., M.E., and S.G. analyzed the data. M.E. and S.G. provided reagents. C.E.G., B.P., M.E., and S.G. wrote the paper. All authors have read and agreed to the published version of the manuscript.

REFERENCES

1. Albert M, Becares M, Falqui M, Fernandez-Lozano C, Guerra S. 2018. ISG15, a small molecule with huge implications: regulation of mitochondrial homeostasis. Viruses 10:629. https://doi.org/10.3390/v10110629.
2. Durfee LA, Huibregtse JM. 2012. The ISG15 conjugation system. Methods Mol Biol 832:141–199. https://doi.org/10.1007/978-1-61779-474-2_9.
3. Villarroya-Beltri C, Baixauli F, Mittelbrunn M, Fernandez-Delgado I, Torralba D, Moreno-Gonzalo O, Baldanta S, Enrich C, Guerra S, Sanchez-Madrid F. 2016. ISGylation controls exosome secretion by promoting lysosomal degradation of MVB proteins. Nat Commun 7:13588. https://doi.org/10.1038/ncomms13588.
4. Villarroya-Beltri C, Guerra S, Sanchez-Madrid F. 2017. ISGylation—a key to lock the cell gates for preventing the spread of threats. J Cell Sci 130:2961–2969. https://doi.org/10.1242/jcs.205468.
5. Ketscher L, Hannß R, Morales DJ, Basters A, Guerra S, Goldmann T, Hausmann A, Prinz M, Naumann R, Pekosz A, Utermöhlen O, Lenschow DJ, Knobeloch K-P. 2015. Selective inactivation of USP18 isopeptidase activity in vivo enhances ISG15 conjugation and viral resistance. Proc Natl Acad Sci U S A 112:1577–1582. https://doi.org/10.1073/pnas.1412881112.
6. Dos Santos PF, Mansur DS. 2017. Beyond ISGlylation: functions of free intracellular and extracellular ISG15. J Interferon Cytokine Res 37:246–253. https://doi.org/10.1089/jir.2016.0103.
7. Zhang Y, Thery F, Wu NC, Luhmann EK, Dussurget O, Foecke M, Bredow C, Jiménez-Fernández D, Leandro K, Beling A, Knobeloch K-P, Impens F, Cossart P, Radoshevich L. 2019. The in vivo ISGylome links ISG15 to metabolic pathways and autophagy upon Listeria monocytogenes infection. Nat Commun 10:5383. https://doi.org/10.1038/s41467-019-13393-x.
8. Kespohl M, Bredow C, Klingel K, Voß M, Paeschke A, Zickler M, Poller W, Kaya Z, Eckstein J, Fechner H, Spranger J, Fähling M, Wirth EK, Rado-

shevich L, Thery F, Impens F, Berndt N, Knobeloch K-P, Beling A. 2020. Protein modification with ISG15 blocks coxsackievirus pathology by antiviral and metabolic reprogramming. Sci Adv 6:eaay1109. https://doi.org/10.1126/sciadv.aay1109.
9. Baldanta S, Fernandez-Escobar M, Acin-Perez R, Albert M, Camafeita E, Jorge I, Vazquez J, Enriquez JA, Guerra S. 2017. ISG15 governs mitochondrial function in macrophages following vaccinia virus infection. PLoS Pathog 13:e1006651. https://doi.org/10.1371/journal.ppat.1006651.
10. Yeh YH, Yang YC, Hsieh MY, Yeh YC, Li TK. 2013. A negative feedback of the HIF-1alpha pathway via interferon-stimulated gene 15 and ISGylation. Clin Cancer Res 19:5927–5939. https://doi.org/10.1158/1078-0432.CCR-13-0018.
11. Swaim CD, Scott AF, Canadeo LA, Huibregtse JM. 2017. Extracellular ISG15 signals cytokine secretion through the LFA-1 integrin receptor. Mol Cell 68:581–590.e5. https://doi.org/10.1016/j.molcel.2017.10.003.
12. Zhang X, Bogunovic D, Payelle-Brogard B, Francois-Newton V, Speer SD, Yuan C, Volpi S, Li Z, Sanal O, Mansouri D, Tezcan I, Rice GI, Chen C, Mansouri N, Mahdaviani SA, Itan Y, Boisson B, Okada S, Zeng L, Wang X, Jiang H, Liu W, Han T, Liu D, Ma T, Wang B, Liu M, Liu JY, Wang QK, Yalnizoglu D, Radoshevich L, Uze G, Gros P, Rozenberg F, Zhang SY, Jouanguy E, Bustamante J, Garcia-Sastre A, Abel L, Lebon P, Notarangelo LD, Crow YJ, Boisson-Dupuis S, Casanova JL, Pellegrini S. 2015. Human intracellular ISG15 prevents interferon-alpha/beta over-amplification and auto-inflammation. Nature 517:89–93. https://doi.org/10.1038/nature13801.
13. Bogunovic D, Byun M, Durfee LA, Abhyankar A, Sanal O, Mansouri D, Salem S, Radovanovic I, Grant AV, Adimi P, Mansouri N, Okada S, Bryant VL, Kong XF, Kreins A, Velez MM, Boisson B, Khalilzadeh S, Ozcelik U, Darazam IA, Schoggins JW, Rice CM, Al-Muhsen S, Behr M, Vogt G, Puel A, Bustamante J, Gros P, Huibregtse JM, Abel L, Boisson-Dupuis S, Casanova JL. 2012. Mycobacterial disease and impaired IFN-gamma immunity in humans with inherited ISG15 deficiency. Science 337:1684–1688. https://doi.org/10.1126/science.1224026.
14. D'Cunha J, Knight E, Jr, Haas AL, Truitt RL, Borden EC. 1996. Immunoregulatory properties of ISG15, an interferon-induced cytokine. Proc Natl Acad Sci U S A 93:211–215. https://doi.org/10.1073/pnas.93.1.211.
15. Padovan E, Terracciano L, Certa U, Jacobs B, Reschner A, Bolli M, Spagnoli GC, Borden EC, Heberer M. 2002. Interferon stimulated gene 15 constitutively produced by melanoma cells induces e-cadherin expression on human dendritic cells. Cancer Res 62:3453–3458.
16. Owhashi M, Taoka Y, Ishii K, Nakazawa S, Uemura H, Kambara H. 2003. Identification of a ubiquitin family protein as a novel neutrophil chemotactic factor. Biochem Biophys Res Commun 309:533–539. https://doi.org/10.1016/j.bbrc.2003.08.038.
17. Napolitano A, van der Veen AG, Bunyan M, Borg A, Frith D, Howell S, Kjaer S, Beling A, Snijders AP, Knobeloch K-P, Frickel E-M. 2018. Cysteine-reactive free ISG15 generates IL-1β-producing CD8α^+ dendritic cells at the site of infection. J Immunol 201:ji1701322. https://doi.org/10.4049/jimmunol.1701322.
18. Villarreal DO, Wise MC, Siefert RJ, Yan J, Wood LM, Weiner DB. 2015. Ubiquitin-like molecule ISG15 acts as an immune adjuvant to enhance antigen-specific CD8 T-cell tumor immunity. Mol Ther 23:1653–1662. https://doi.org/10.1038/mt.2015.120.
19. Iglesias-Guimarais V, Ahrends T, de Vries E, Knobeloch KP, Volkov A, Borst J. 2020. IFN-stimulated gene 15 is an alarmin that boosts the CTL response via an innate, NK cell-dependent route. J Immunol 204:2110–2121. https://doi.org/10.4049/jimmunol.1901410.
20. Perez P, Marin MQ, Lazaro-Frias A, Sorzano COS, Gomez CE, Esteban M, Garcia-Arriaza J. 2020. Deletion of vaccinia virus A40R gene improves the immunogenicity of the HIV-1 vaccine candidate MVA-B. Vaccines (Basel) 8:70. https://doi.org/10.3390/vaccines8010070.
21. García-Arriaza J, Nájera JL, Gómez CE, Tewabe N, Sorzano COS, Calandra T, Roger T, Esteban M. 2011. A candidate HIV/AIDS vaccine (MVA-B) lacking vaccinia virus gene C6L enhances memory HIV-1-specific T-cell responses. PLoS One 6:e24244. https://doi.org/10.1371/journal.pone.0024244.
22. García-Arriaza J, Nájera JL, Gómez CE, Sorzano COS, Esteban M. 2010. Immunogenic profiling in mice of a HIV/AIDS vaccine candidate (MVA-B) expressing four HIV-1 antigens and potentiation by specific gene deletions. PLoS One 5:e12395. https://doi.org/10.1371/journal.pone.0012395.
23. García-Arriaza J, Gómez CE, Sorzano CÓS, Esteban M. 2014. Deletion of the vaccinia virus N2L gene encoding an inhibitor of IRF3 improves the immunogenicity of modified vaccinia virus Ankara expressing HIV-1 antigens. J Virol 88:3392–3410. https://doi.org/10.1128/JVI.02723-13.
24. Garcia-Arriaza J, Arnaez P, Gomez CE, Sorzano CO, Esteban M. 2013. Improving adaptive and memory immune responses of an HIV/AIDS vaccine candidate MVA-B by deletion of vaccinia virus genes (C6L and K7R) blocking interferon signaling pathways. PLoS One 8:e66894. https://doi.org/10.1371/journal.pone.0066894.
25. Rerks-Ngarm S, Pitisuttithum P, Nitayaphan S, Kaewkungwal J, Chiu J, Paris R, Premsri N, Namwat C, de Souza M, Adams E, Benenson M, Gurunathan S, Tartaglia J, McNeil JG, Francis DP, Stablein D, Birx DL, Chunsuttiwat S, Khamboonruang C, Thongcharoen P, Robb ML, Michael NL, Kunasol P, Kim JH, MOPH-TAVEG Investigators. 2009. Vaccination with ALVAC and AIDSVAX to prevent HIV-1 infection in Thailand. N Engl J Med 361:2209–2220. https://doi.org/10.1056/NEJMoa0908492.
26. Liu J, Ostrowski M. 2017. Development of targeted adjuvants for HIV-1 vaccines. AIDS Res Ther 14:43. https://doi.org/10.1186/s12981-017-0165-8.
27. Tecalco Cruz AC, Mejia-Barreto K. 2017. Cell type-dependent regulation of free ISG15 levels and ISGylation. J Cell Commun Signal 11:127–135. https://doi.org/10.1007/s12079-017-0385-7.
28. Knight E, Jr, Cordova B. 1991. IFN-induced 15-kDa protein is released from human lymphocytes and monocytes. J Immunol 146:2280–2284.
29. Perng YC, Lenschow DJ. 2018. ISG15 in antiviral immunity and beyond. Nat Rev Microbiol 16:423–439. https://doi.org/10.1038/s41579-018-0020-5.
30. Campbell JA, Lenschow DJ. 2013. Emerging roles for immunomodulatory functions of free ISG15. J Interferon Cytokine Res 33:728–738. https://doi.org/10.1089/jir.2013.0064.
31. Wood LM, Pan ZK, Seavey MM, Muthukumaran G, Paterson Y. 2012. The ubiquitin-like protein, ISG15, is a novel tumor-associated antigen for cancer immunotherapy. Cancer Immunol Immunother 61:689–700. https://doi.org/10.1007/s00262-011-1129-9.
32. Wang RG, Kaul M, Zhang DX. 2012. Interferon-stimulated gene 15 as a general marker for acute and chronic neuronal injuries. Sheng Li Xue Bao 64:577–583.
33. Gomez CE, Najera JL, Jimenez EP, Jimenez V, Wagner R, Graf M, Frachette MJ, Liljestrom P, Pantaleo G, Esteban M. 2007. Head-to-head comparison on the immunogenicity of two HIV/AIDS vaccine candidates based on the attenuated poxvirus strains MVA and NYVAC co-expressing in a single locus the HIV-1BX08 gp120 and HIV-1(IIIB) Gag-Pol-Nef proteins of clade B. Vaccine 25:2863–2885. https://doi.org/10.1016/j.vaccine.2006.09.090.
34. Ramirez JC, Gherardi MM, Esteban M. 2000. Biology of attenuated modified vaccinia virus Ankara recombinant vector in mice: virus fate and activation of B- and T-cell immune responses in comparison with the Western Reserve strain and advantages as a vaccine. J Virol 74:923–933. https://doi.org/10.1128/jvi.74.2.923-933.2000.
35. Tscharke DC, Woo WP, Sakala IG, Sidney J, Sette A, Moss DJ, Bennink JR, Karupiah G, Yewdell JW. 2006. Poxvirus CD8$^+$ T-cell determinants and cross-reactivity in BALB/c mice. J Virol 80:6318–6323. https://doi.org/10.1128/JVI.00427-06.
36. Gomez CE, Najera JL, Jimenez V, Bieler K, Wild J, Kostic L, Heidari S, Chen M, Frachette MJ, Pantaleo G, Wolf H, Liljestrom P, Wagner R, Esteban M. 2007. Generation and immunogenicity of novel HIV/AIDS vaccine candidates targeting HIV-1 Env/Gag-Pol-Nef antigens of clade C. Vaccine 25:1969–1992. https://doi.org/10.1016/j.vaccine.2006.11.051.
37. Nájera JL, Gómez CE, García-Arriaza J, Sorzano CO, Esteban M. 2010. Insertion of vaccinia virus C7L host range gene into NYVAC-B genome potentiates immune responses against HIV-1 antigens. PLoS One 5:e11406. https://doi.org/10.1371/journal.pone.0011406.